Hindawi
Journal of Sensors
Volume 2017, Article ID 9591081, 6 pages
https://doi.org/10.1155/2017/9591081

Research Article

Structure-Dependent CO_2 Gas Sensitivity of $La_2O_2CO_3$ Thin Films

Margus Kodu, Tea Avarmaa, Hugo Mändar, Rando Saar, and Raivo Jaaniso

Institute of Physics, University of Tartu, W. Ostwald St 1, 50411 Tartu, Estonia

Correspondence should be addressed to Raivo Jaaniso; raivo.jaaniso@ut.ee

Received 27 February 2017; Accepted 4 June 2017; Published 11 July 2017

Academic Editor: Sang Sub Kim

Rare earth oxycarbonates are potential candidate materials for constructing simple and low-cost chemiresistive sensors for monitoring carbon dioxide (CO_2) gas in the living and working environment for personal comfort and health reasons. Also, measurement of CO_2 concentrations is needed in many industrial processes. Specifically, sol-gel made nanoparticles of Nd and La oxycarbonates have been studied previously as novel CO_2 gas sensor materials. In this paper, pulsed laser deposition of La oxycarbonate ($La_2O_2CO_3$) thin films was studied and structural properties of obtained thin films were characterized. Also, CO_2 gas sensing ability of synthesized films was evaluated. The films deposited under CO_2 partial pressure in various conditions were all Raman amorphous. In situ or ex situ annealing procedure at high CO_2 partial pressure was needed for obtaining crystalline $La_2O_2CO_3$ films, whereby hexagonal and monoclinic polymorphs were obtained in ex situ and in situ processes, respectively. Sensor structure, made using in situ process, was sensitive to CO_2 gas and showed relatively fast response and recovery characteristics.

1. Introduction

CO_2 is one of the harmful pollutant gases in closed rooms and also in the environment. Therefore, there is a demand for effective methods for monitoring CO_2 levels. Current industrially available CO_2 sensors are relatively complex and expensive, so it is desirable to develop simple and low-cost methods for monitoring CO_2 level [1]. La and Nd oxycarbonates have recently been studied as promising candidates for chemiresistive CO_2 sensor materials [2–6]. However, in these reports, La and Nd oxycarbonates have been studied in a form of nanorods and there are no investigations of thin film deposition of these promising materials for CO_2 gas sensor application. In [2–5], La and Nd oxycarbonate materials were made using respective precursor hydroxides in a form of nanoparticles prepared in a sol-gel process. Conversion of La and Nd hydroxide nanorods to respective oxycarbonates was carried out by heating the materials in the atmosphere containing CO_2 gas.

Within the class of oxycarbonate materials, pulsed laser deposition (PLD) has been used for the synthesis of Ba-Ca-Cu, Sr-Cu, and Ba-Sr-Cu oxycarbonate thin films, which have been studied as superconductors [7–10]. In all of these reports [7–10], pure oxide materials were used as pulsed laser deposition targets. Oxycarbonate thin films were obtained by postdeposition furnace annealing [8] or by in situ annealing of deposited films at higher gas pressure [7, 9, 10].

In general, rare earth oxycarbonates are stable compounds in ambient conditions. Their synthesis, thermal stability, and crystalline modifications (metastable polymorphs (I) tetragonal, (Ia) monoclinic, and (II) hexagonal) are described in [11–14].

In this work, lanthanum oxycarbonate thin films were deposited using $La_2O_2CO_3$ ceramic targets. Two different postgrowth treatments for obtaining crystalline $La_2O_2CO_3$ films were used. Obtained films were characterized by electron microscopy, X-ray diffraction, and Raman spectroscopy methods. CO_2 gas sensing capability of grown $La_2O_2CO_3$ films was demonstrated.

2. Materials and Methods

Lanthanum oxycarbonate films with ~180 nm thickness were deposited by PLD method on two types of substrates: (a) $Si(100)/SiO_2$ (25 nm thermal oxide) substrates for structural

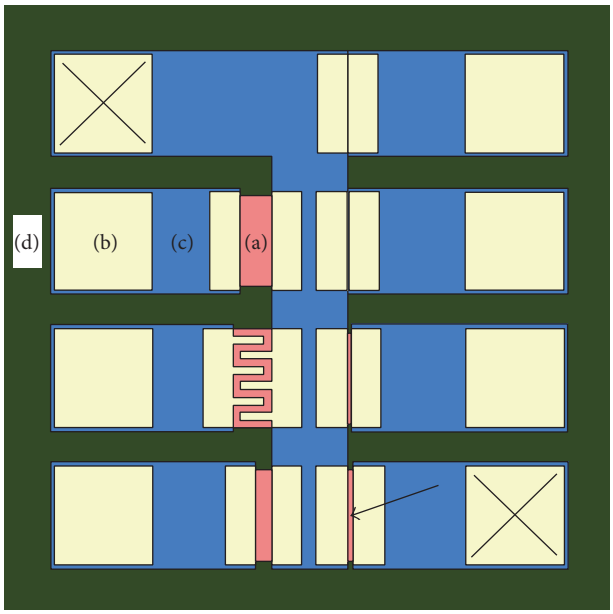

Figure 1: The scheme ("aerial view") of the microelectrode substrate. Its lateral dimensions are $4 \times 4\,mm^2$. The letters ((a), (b), (c), and (d)) and corresponding halftones are indicating the exposed materials: (a) passivated substrate (Si + SiO_xN_y 200 nm); (b) electrodes (Ti 10 nm + Pt 250 nm) on (a); (c) SiO_xN_y 1800 nm on (b); (d) SiO_xN_y 1800 nm on (a). The slit used for sensor measurements is marked with an arrow and the contact pads for this slit are marked with crosses.

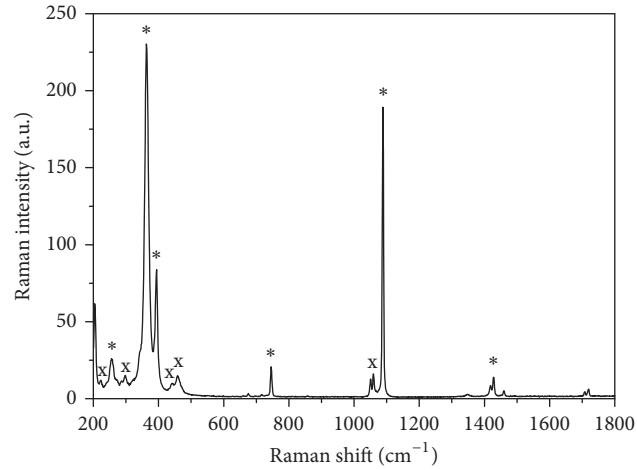

Figure 2: Raman spectrum of $La_2O_2CO_3$ PLD target. The marked Raman peaks correspond to monoclinic (x) or hexagonal (∗) $La_2O_2CO_3$. All unmarked peaks belong also to hexagonal phase.

characterization and (b) Windsor Scientific SM160 microelectrode substrates with Pt electrodes (Figure 1). SM160 has seven independently addressable electrode pairs with different electrode separation distances ranging from 4 to 200 μm (a-type areas in Figure 1). The length of six electrode gaps is 0.6 mm. Films were deposited onto electrode substrate using a stainless steel mask that left open only the central part of the substrate. Mask ensured that no film was deposited onto contact pads. Prior to deposition, the substrates were cleaned by processing in an ultrasonic bath in acetone and rinsing in acetone and methanol. $La_2O_2CO_3$ ceramic targets were made from $La_2(CO_3)_3 * 6H_2O$ (purity 99,9%) powder, which was dried in vacuum oven at 200°C during 24 h and pressed into pellets at 400 MPa. Following thermal treatment of pellets was carried out in two steps: (1) the temperature was raised slowly up to 500°C in air and (2) the pellets were sintered in CO_2 and O_2 gas mixture (1 : 9) at 800°C for 15 h. A KrF excimer laser (COMPexPro 205, Coherent; wavelength 248 nm, pulse width 25 ns) was used for PLD. During deposition of $La_2O_2CO_3$ films, the energy density of laser pulse on the target was 1.5 J/cm^2, the pulse repetition rate was 10 Hz, and the distance between the substrate and the target was 7.5 cm. Pure CO_2 or O_2/10% CO_2 background gas at 10^{-2} or 10^{-1} mbar pressure was used during the deposition process. The substrate temperature was varied between 300 and 700°C. Other details of the deposition process are described elsewhere [15]. Two types of annealing procedures were used for after-growth processing of the films: (a) ex situ annealing or (b) in situ annealing process. Ex situ annealing was carried out in a tube furnace at 550°C for 30 min in flowing humidified O_2/10% CO_2 gas mixture at normal pressure. Humidification was realized by guiding the gas mixture through the distilled water. In situ annealing was carried out immediately after the PLD process in the deposition chamber under the CO_2 gas atmosphere at the pressure of 7 mbar and at the temperature of 660°C. In situ annealing time was 30 min.

The structure of the deposited films was characterized by grazing incidence X-ray diffraction (GIXRD, incidence angle 0.5°), scanning electron microscopy (SEM), Raman spectroscopy, and spectroscopic ellipsometry. The measurements of electrical and gas response characteristics were carried out with a Keithley 2400 SourceMeter, a gas mixing system based on five Brooks mass flow controllers, and a sample chamber with small hotplate heater (see [16]). A mixture of N_2 and O_2 gases (both 99.999% pure) was used as a carrier gas. The source of CO_2 additive was a mixture of 10% CO_2 in O_2 (99.999% pure). The oxygen concentration (21%) and the flow rate (200 ml/min) of the gas mixture were kept constant during the measurements.

3. Results and Discussion

Figure 2 depicts the Raman spectrum of a PLD target synthesized using pure lanthanum carbonate $La_2(CO_3)_3 * 6H_2O$. The Raman bands in this spectrum can be attributed either to monoclinic or to hexagonal $La_2O_2CO_3$, which are commonly observed La oxycarbonate crystal phases and are generally marked as phase (Ia) and phase (II), respectively. Both polymorphs have their distinctive bands in the Raman spectrum. (II) $La_2O_2CO_3$ is characterized by intense bands at 363 and 393 cm^{-1}, along with a sharp band at 1088 cm^{-1}. (Ia) $La_2O_2CO_3$ can be easily identified by two bands at 1050 and 1060 cm^{-1} [17]. All intense peaks in the spectrum of PLD target shown in Figure 2 belong to (II) $La_2O_2CO_3$ phase.

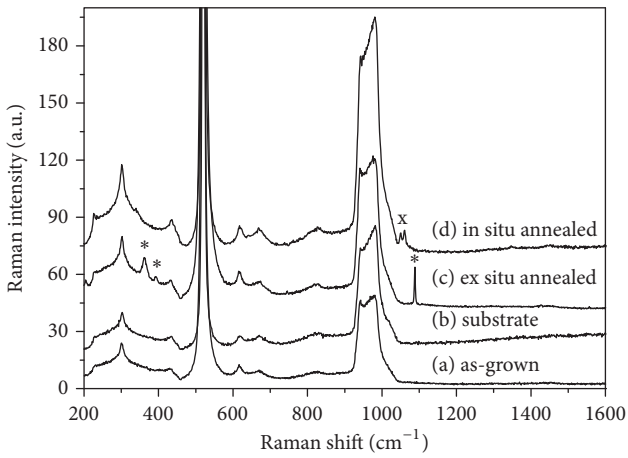

FIGURE 3: Raman spectra of as-grown and annealed films. The marked Raman peaks correspond to monoclinic (x) or hexagonal (∗) $La_2O_2CO_3$. All unmarked peaks originate from the substrate.

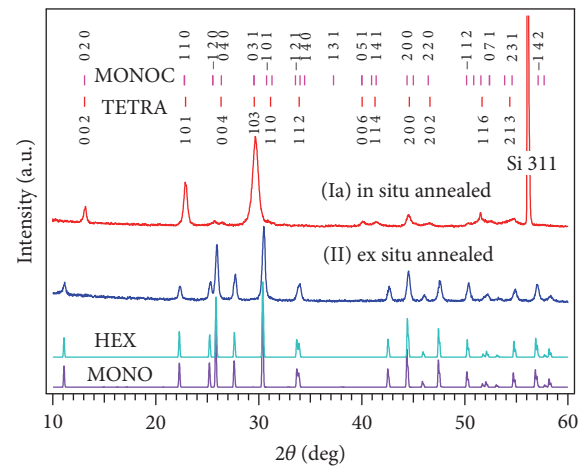

FIGURE 4: X-ray diffraction patterns of ex situ and in situ annealed films showing hexagonal or monoclinic polymorph of ex situ annealed film and monoclinic structure of in situ annealed film. A pattern denoted as MONO is calculated for monoclinic phase (ICSD collection code 51468), HEX is calculated for hexagonal phase (ICSD collection code 202988), TETRA denotes the peak positions together with their Miller indices of tetragonal phase (ICDD PDF-2 file number 23-0320), and MONOC denotes the peak positions together with Miller indices of monoclinic phase (ICDD PDF-2 file number 48-1113).

However, weaker bands at 1050 and 1060 cm^{-1} indicate the presence of Ia type minority polymorph in the target. This is supported also by four weak bands appearing at 223, 297, 442, and 458 cm^{-1} in the spectrum, which can all be attributed to the monoclinic $La_2O_2CO_3$ phase. Therefore, according to Raman analysis, our PLD target consisted mainly of hexagonal $La_2O_2CO_3$ with only small traces of monoclinic phase. No indication of any other phases, for example, La oxide or La hydroxide phases, was found in Raman analysis. It has to be noted that the coexistence of type (Ia) and (II) $La_2O_2CO_3$ phases is a previously known phenomenon and at equilibrium conditions type Ia transforms to type (II) at temperatures over 400°C [12, 17].

According to the analysis of Raman spectra, thin films grown at various deposition conditions were all amorphous and showed no Raman peaks. Ex situ or in situ annealing at higher CO_2 partial pressure was needed for film crystallization. This is illustrated in Figure 3 where (a) is the spectrum of the film grown at 500°C using O_2/10% CO_2 gas mixture at 5×10^{-2} mbar. Raman bands characteristic to $La_2O_2CO_3$ are absent in graph (a) of Figure 3. Only Raman peaks originating from Si/SiO_2 substrate can be seen. This is easily confirmed by comparing with spectrum taken from a pure substrate, graph (b). Graphs (c) and (d) depict Raman spectra of ex situ and in situ annealed thin films, respectively. Raman spectrum of the film annealed ex situ at 550°C (Figure 3(c)) has a clear band at 1088 cm^{-1}, which is characteristic for hexagonal $La_2O_2CO_3$ phase. In addition, Raman spectrum in Figure 3(c) also contains two weak Raman bands at 362 and 393 cm^{-1} which can be assigned to (II) $La_2O_2CO_3$ phase. The spectrum of the film annealed in situ at 660°C (Figure 3(d)) shows two clear peaks at 1050 and 1060 cm^{-1}, which belong to monoclinic $La_2O_2CO_3$ phase. Spectrum (d) contains also a weak band at 224 cm^{-1} assignable to monoclinic phase.

XRD analysis of ex situ and in situ annealed films, in general, confirmed the results of Raman spectroscopy. XRD patterns are depicted in Figure 4. Both diffraction patterns can be assigned to crystalline $La_2O_2CO_3$, whereas the peaks originating from ex situ and in situ annealed films can be attributed to hexagonal II (ICDD PDF-2 file number 37-0804, space group P63/mmc) or monoclinic (ICDD PDF-2 file number 01-70-5540, space group C12/c1) and tetragonal (ICDD PDF-2 file number 23-0320, space group I4/mmm) or monoclinic (ICDD PDF-2 file number 48-1113, space group unknown) phases, respectively. XRD pattern cannot distinguish between hexagonal and monoclinic phases of ex situ annealed film because both phases show quite similar diffraction patterns (Figure 4, patterns denoted as HEX and MONOC). The space groups P63/mmc and C12/c1 can be distinguished only by very weak extra reflections of monoclinic phase that cannot be detected because of a low average intensity of observed diffraction patterns. However, it is important to note that the monoclinic polymorph is just more refined model structure of type (II) $La_2O_2CO_3$ [18]. Typically, only average, hexagonal, model of type (II) polymorph is considered since it cannot be distinguished from monoclinic polymorph by applying typical experimental setups for structural analysis. Therefore, it is reasonable to consider that our ex situ annealed films consist of type (II) hexagonal La oxycarbonate crystal phase.

The monoclinic phase is the preferred assignment over tetragonal phase for in situ annealed films because the former gave a better match for all weak reflections in the following ranges of XRD pattern: 25–27°, 30.7–38.7°, and 49–59° (Figure 3). However, it cannot be completely ruled out that some amount of tetragonal phase is present in in situ annealed films. A strong and sharp XRD peak near 56° originates from the substrate and can be assigned to reflection

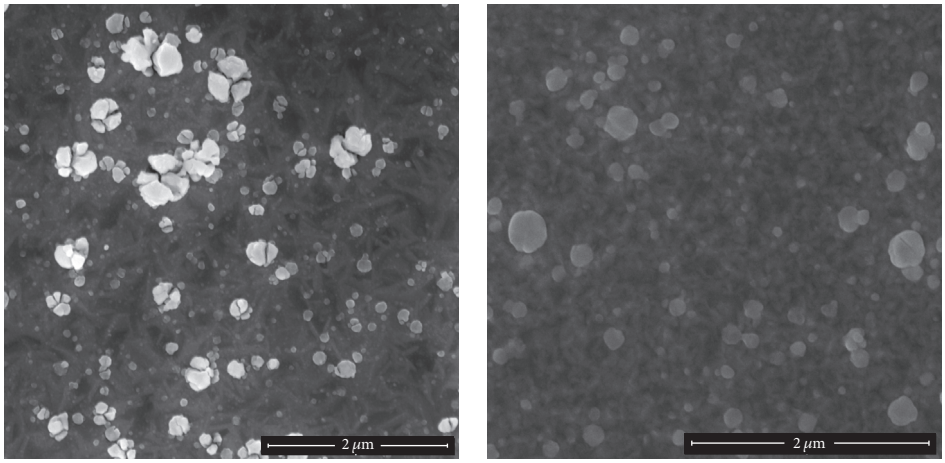

(a) SEM image of ex situ annealed $La_2O_2CO_3$ film (b) SEM image of in situ annealed $La_2O_2CO_3$ film

Figure 5

311 of Si (diffraction angle is 56.12° according to ICDD PDF-2 file number 27-1402).

SEM images of in situ and ex situ annealed $La_2O_2CO_3$ films are shown in Figure 5. Crystallite grains of film material are clearly noticeable in the SEM images. Also, it can be seen from the SEM images that both films have relatively high concentration of particulates with sizes up to 350 nm in diameter. Note that the average thickness of the films is approximately 180 nm. Micro- and nanoparticle production during PLD process is a usual phenomenon [19, 20]. These particles are formed either from solidified liquid droplets that are expelled from the target during laser-target interaction process or by nucleation and growth of nanoparticles in propagating plasma plume of gas phase species [19]. Droplets originating from the target have typical sizes in the micron or submicron range, while the sizes of the particulates created in PLD plasma are in the nanometer range. The quantity of particulates could possibly be reduced by optimizing process parameters, such as laser fluence and background gas pressure. A noticeable feature is that the particulates in the SEM image of ex situ annealed film (Figure 5(a)) are split into two or more parts, while the particulates in the image of in situ annealed film (Figure 5(b)) are intact. The splitting of particulates is probably related to the hydroxylation and partial carbonation of La_2O_3, which is probably the phase of as-grown films (see discussion below), under ambient atmosphere. As reports of SEM images of oxycarbonate films are scarce, we cannot compare the appearance of our $La_2O_2CO_3$ films with previously obtained results.

Gas sensor measurements were made at 450°C, with CO_2 gas concentrations of 750 and 1500 ppm. Relative humidity of the test gas was 21%. The measurements were made using the electrodes with 48 μm gap width and 0.6 mm gap length. The current through the sample was monitored at the applied constant voltage of 3 V. Previously, it is reported that the sensor structures based on La and Nd oxycarbonate nanorods have high electrical resistivity and that restrict their use in commercial sensors [2–4]. In our sensor structures, the resistivity followed the Arrhenius law with an activation energy of 0.56 eV between 250 and 450°C. It shows that the conductivity is determined by deep trap levels, as the bandgap of the material, as concluded from X-ray absorption spectroscopy and X-ray emission spectroscopy studies by Hirsch et al. [6], is approximately 3.7 eV in the case of $La_2O_2CO_3$ nanoparticles. At 250°C, the resistivity was at the limit of our detection capability as the detected current was slightly below 1 nA. Reasonable signal and fastest response times were obtained at the highest temperature probed, at 450°C, when the resistivity of the material was 340 Ω·m. Time transients of the CO_2 gas response of in situ annealed sensor structure are depicted in Figure 6. It can be seen that the relative gas response to 1500 ppm of CO_2 is about 2.2; that is, the measured current decreased from 2.4×10^{-8} to 1.1×10^{-8} A. The response and recovery times of the sensor signal, determined as the times at which the 90% level of the final

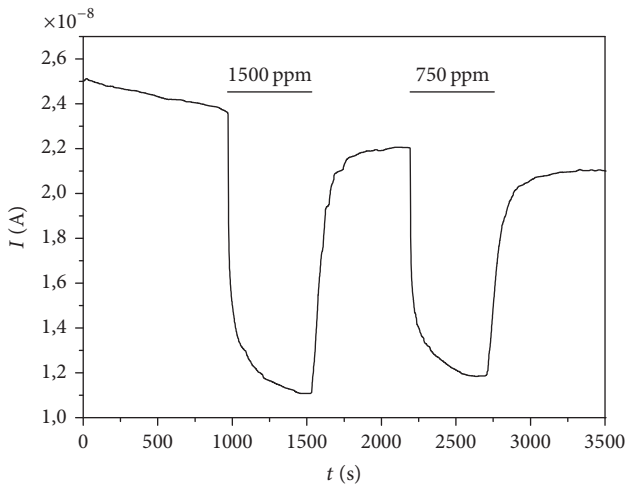

Figure 6: Temporal responses of sensor current (at applied voltage of 3 V) to 1500 and 750 ppm of CO_2 gas.

signal were achieved, are 165 s and 189 s, respectively. Our thin film sensor structures have considerably faster responses as compared to sensors based on La and Nd oxycarbonate nanorods [2–5]. It is especially notable in the case of recovery times, which have been found to be over 30 min in [2–5].

According to Hirsch et al. [6], CO_2 adsorbing onto monoclinic $La_2O_2CO_3$ interacts directly with La site on the surface and forms surface carbonate at the site of absorption. Adsorbing CO_2 acts as an electron acceptor, thus reducing the concentration of free electrons and causing an increase of resistivity of the sensor material. Also, recent studies indicate that surface hydroxyl groups play important role in CO_2 adsorption at $La_2O_2CO_3$, but exact mechanism and the role of OH groups are not known [4, 6].

The difference between the films obtained by in situ and ex situ annealing procedures can be explained as follows. As discussed in the works of Orera et al. and Bakiz et al. [17, 21], the La_2O_3-H_2O-CO_2 ternary system is relatively complex. The phases obtained in different experiments and described in the literature vary and depend considerably on the thermal history of the sample and various experimental conditions. However, our results can be clearly interpreted based on the results and discussion of the paper by Orera et al. [17]. According to Raman analysis, our as-grown films do not contain crystalline phases. It can be presumed that the CO_2 pressure that was used during the film growth was not sufficient for the formation of a stable oxycarbonate phase. It can be supposed that the as-grown film consists mainly of amorphous lanthanum oxide but it may also be partially carbonated to form a $La_xO_y(CO_3)_z$ type nonstoichiometric amorphous phase. When deposited film is taken out from the deposition chamber, it gets into the contact with H_2O and CO_2 in ambient air. When La_2O_3 is in contact with ambient air, it rapidly forms $La(OH)_3$. According to previous literature reports [17, 22, 23], the aging of $La(OH)_3$ in air at room temperature (RT) results in the formation of partially hydrated carbonates of $La_x(OH)_y(CO_3)_z$ type. In [17], the aging of $La(OH)_3$ material at RT in ambient air was followed by annealing at 400°C, and, as a result, the sample was crystallized into pure hexagonal $La_2O_2CO_3$ phase. However, when the high-temperature annealing was performed with $La(OH)_3$, that is, without longer aging of the material at RT, the authors found, as a final product, monoclinic type $La_2O_2CO_3$. The carbonization of La_2O_3 under CO_2 flow was also studied in [21]. The transformation of La_2O_3 to monoclinic type $La_2O_2CO_3$ was observed at the temperatures around 525°C. Our results are in agreement with these previous outcomes as our ex situ annealed films, which got into contact with ambient air, were crystallized into hexagonal phase. In addition, if our laser deposited film was annealed in situ, without exposing it to ambient air, monoclinic $La_2O_2CO_3$ was obtained.

4. Conclusions

La oxycarbonate thin films were obtained by pulsed laser deposition and postannealing in CO_2 containing atmosphere using ceramic $La_2O_2CO_3$ target. The structure of as-deposited films was amorphous. In order to obtain crystalline oxycarbonate films, in situ or ex situ annealing under high CO_2 partial pressure was necessary. The type of crystalline La oxycarbonate phase depended on annealing method as hexagonal, or type (II) phase was obtained by ex situ annealing and monoclinic phase, or type Ia was obtained by in situ annealing procedure. The main difference between two annealing methods was that the films, subjected to ex situ annealing, got into contact with atmospheric water vapor. Two different routes for obtaining $La_2O_2CO_3$ films in this work can schematically be described as follows: (a) ex situ annealing: $La_2O_3 \rightarrow La(OH)_3 \rightarrow La_x(OH)_y(CO_3)_z \rightarrow$ hexagonal $La_2O_2CO_3$; (b) in situ annealing: $La_2O_3 \rightarrow$ monoclinic $La_2O_2CO_3$. The films obtained by in situ annealing showed a relatively fast conductometric response to CO_2 gas in the actual concentration range (400–2000 ppm). The conductivity of 180 nm thick thin films in the pure synthetic air was 2.9 mS/m and it decreased over 2 times under the influence of 1500 ppm of CO_2. The gas response and recovery times determined at 450°C were within 165–189 s.

Disclosure

The preliminary results have been presented at the E-MRS 2015 Fall Meeting.

Conflicts of Interest

The authors declare that they have no conflicts of interest.

Acknowledgments

This study was supported by Estonian Research Council (Institutional Projects IUT34-27 and IUT2-24) and by European Regional Development Fund (SA Archimedes Project 3.2.1101.12-0014). The authors gratefully thank Aare Floren for help with technical problems.

References

[1] R. Jaaniso and O. K. Tan, *Semiconductor Gas Sensors*, Elsevier, 2013.

[2] G. Chen, B. Han, S. Deng, Y. Wang, and Y. Wang, "Lanthanum dioxide carbonate $La_2O_2CO_3$ nanorods as a sensing material for chemoresistive CO_2 gas sensor," *Electrochimica Acta*, vol. 127, pp. 355–361, 2014.

[3] A. Haensch, D. Borowski, N. Barsan, D. Koziej, M. Niederberger, and U. Weimar, "Faster response times of rare-earth oxycarbonate based CO_2 sensors and another readout strategy for real-world applications," *Procedia Engineering*, vol. 25, pp. 1429–1432, 2011.

[4] I. Djerdj, A. Haensch, D. Koziej et al., "Neodymium dioxide carbonate as a sensing layer for chemoresistive CO_2 sensing," *Chemistry of Materials*, vol. 21, no. 22, pp. 5375–5381, 2009.

[5] A. Haensch, D. Koziej, M. Niederberger, N. Barsan, and U. Weimar, "Rare earth oxycarbonates as a material class for chemoresistive CO_2 gas sensors," *Procedia Engineering*, vol. 5, pp. 139–142, 2010.

[6] O. Hirsch, K. O. Kvashnina, L. Luo, M. J. Süess, P. Glatzel, and D. Koziej, "High-energy resolution X-ray absorption and emission

spectroscopy reveals insight into unique selectivity of La-based nanoparticles for CO_2," *Proceedings of the National Academy of Sciences of the United States of America*, vol. 112, no. 52, pp. 15803–15808, 2015.

[7] G. Calestani, A. Migliori, U. Spreitzer et al., "Ba-Ca-Cu oxycarbonate thin films, prepared by pulsed laser deposition: structure, growth mechanism and superconducting properties," *Physica C: Superconductivity and its Applications*, vol. 312, no. 3-4, pp. 225–232, 1999.

[8] R. Feenstra, J. D. Budai, D. K. Christen, and T. Kawai, "Superconductivity in epitaxial films of the oxycarbonate $Sr_2CuO_2(CO_3)$ converted from "infinite layer" $SrCuO_2$ by thermal processing," *Applied Physics Letters*, vol. 67, p. 1310, 1995.

[9] W. Prellier, A. Tebano, J. L. Allen et al., "$Ba_{2-x}Sr_xCuO_2CO_3$: a series of oxycarbonate thin films grown by pulsed laser deposition on NdGaO3 substrates," *Chemistry of Materials*, vol. 9, no. 1, pp. 319–327, 1997.

[10] W. Prellier, B. Mercey, P. Lecoeur, J. F. Hamet, and B. Raveau, "Tailored superlattices containing distinct oxide and oxycarbonate blocks grown by pulsed laser deposition," *Applied Physics Letters*, vol. 71, no. 6, pp. 782–784, 1997.

[11] J. O. Sawyer, P. Caro, and L. Eyring, "Herstellung, Analyse und röntgenographische Identifizierung der Dioxymonocarbonate des Lanthans und der Lanthanidenelemente," *Monatshefte für Chemie*, vol. 103, no. 1, pp. 333–354, 1972.

[12] R. P. Turcotte, J. O. Sawyer, and L. Eyring, "On the rare earth dioxymonocarbonates and their decomposition," *Inorganic Chemistry*, vol. 8, no. 2, pp. 238–246, 1969.

[13] J. Hölsä and T. Turkki, "Preparation, thermal stability and luminescence properties of selected rare earth oxycarbonates," *Thermochimica Acta*, vol. 190, no. 2, pp. 335–343, 1991.

[14] A. Olafsen and H. Fjellvåg, "Synthesis of rare earth oxide carbonates and thermal stability of $Nd_2O_2CO_3$ II," *Journal of Materials Chemistry*, vol. 9, no. 10, pp. 2697–2702.

[15] E. Feldbach, R. Jaaniso, M. Kodu et al., "Luminescence characterization of ultrathin MgO films of high crystallinity prepared by pulsed laser deposition," *Journal of Materials Science: Materials in Electronics*, vol. 20, no. 1, pp. S321–S325, 2009.

[16] M. Kodu, T. Avarmaa, A. Floren, and R. Jaaniso, "Bias dependent NO2 sensitivity of SnO2 thin films at room temperature," *Journal of the European Ceramic Society*, vol. 33, no. 12, pp. 2335–2340, 2013.

[17] A. Orera, G. Larraz, and M. L. Sanjuán, "Spectroscopic study of the competition between dehydration and carbonation effects in La_2O_3-based materials," *Journal of the European Ceramic Society*, vol. 33, no. 11, pp. 2103–2110, 2013.

[18] A. Olafsen, A.-K. Larsson, H. Fjellvåg, and B. C. Hauback, "On the crystal structure of Ln2O2CO3 II (Ln=La and Nd)," *Journal of Solid State Chemistry*, vol. 158, no. 1, pp. 14–24, 2001.

[19] D. B. Chriesy and G. K. Hubler, *Pulsed Laser Deposition of Thin Films*, John Wiley & Sons, New York, NY, USA, 1994.

[20] P. R. Willmott and J. R. Huber, "Pulsed laser vaporization and deposition," *Reviews of Modern Physics*, vol. 72, no. 1, pp. 315–328, 2000.

[21] B. Bakiz, F. Guinneton, M. Arab et al., "Carbonatation and decarbonatation kinetics in the La_2O_3-$La_2O_2CO_3$ system under CO_2 gas flows," *Advances in Materials Science and Engineering*, vol. 2010, Article ID 360597, 6 pages, 2010.

[22] S. Bernal, F. J. Botana, R. García, and J. M. Rodríguez-Izquierdo, "Thermal evolution of a sample of La_2O_3 exposed to the atmosphere," *Thermochimica Acta*, vol. 66, no. 1–3, pp. 139–145, 1983.

[23] S. Bernal, J. A. Díaz, R. García, and J. M. Rodríguez-Izquierdo, "Study of some aspects of the reactivity of La_2O_3 with CO_2 and H_2O," *Journal of Materials Science*, vol. 20, no. 2, pp. 537–541, 1985.